Available online at www.CivileJournal.org

Civil Engineering Journal

(E-ISSN: 2476-3055; ISSN: 2676-6957)

Vol. 10, No. 08, August, 2024

Experimental Study on the Effect of Flow Velocity and Slope on Stream Bank Stability (Part I)

Jawad Kadhim [1*], Mohanned Q. Waheed [1], Haitham A. Hussein [2], Saad F. A. Al-Wakel [1]

[1] *Department of Civil Engineering, University of Technology-Iraq, Baghdad, Iraq.*

[2] *Department of Civil Engineering, Al-Nahrain University, Baghdad, Iraq.*

Received 22 April 2024; Revised 17 July 2024; Accepted 24 July 2024; Published 01 August 2024

Abstract

The erosion of riverbanks is a significant and capricious national concern. The Al Muwahada channel in Iraq experiences instability in its banks, resulting in failure, retreat, and morphological alterations. These issues are mostly caused by factors such as the velocity of the flow, the angle of the slope, and type of soil. This study investigated the behavior of canal bank soil in response to erosion and variations in slope angle. Therefore, a physical model of a case study was established in the laboratory. Additionally, a slope angle of 26˚ is being utilized, which has not been previously studied in the laboratory. This angle will be tested with five different velocity values: 0.101 m/s, 0.116 m/s, 0.12 m/s, 0.13 m/s, and 0.135 m/s. The bank's deformation was measured for a period of 12 hours, which was divided into 4 equal intervals for each velocity. The study determined that a riverbank with a slope of 26˚ is more resistant to erosion when the velocity of the water is below 0.12 m/s. Velocities equal to or greater than 0.12 m/s have a substantial impact on the erosion of the riverbed. According to this study, a velocity of 0.12 m/s or higher leads to increased erosion of the riverbank. This is equivalent to a velocity of 0.804 m/s in the prototype channel. The section of the riverbank that has suffered the greatest damage due to erosion is the upper two-thirds. The used methodology supports global efforts to increase information about the behavior of river banks with unexplored rivers that have different flow velocities and bank slope angles.

Keywords: Erosion; Riverbank; Slope Angle; Velocity of Flow; Sediment; River Banks.

1. Introduction

Riverbank erosion is the phenomenon in which soil is displaced or transported away from the riverbanks because of the hydraulic force exerted by the water. The causes of this phenomenon can be attributed to various elements, such as the velocity of the flow, the kind of soil on the bank, and the angle of the bank slope. Additionally, human activities such as development near the river or deforestation [1-3]. The primary factor responsible for flow-induced bank erosion is the erosive force of water that is flowing, such as in rivers or coastal currents. Flow-induced bank erosion occurs when the energy of the water exceeds the resistance of the bank materials [4-5]. Erosion can be caused by various factors, such as increased water velocity, increased flow, and the presence of silt, which can all act in combination. Over an extended period, the continuous flow of water progressively erodes the banks, resulting in their eventually being removed [6]. Deng et al. [7] conducted numerical simulations to analyze the seepage and stress variations in the riverbank. The results of the simulation and field observation indicate that the erosion of the protected riverbank is mostly caused by near-bank flow-induced hydraulic erosion. The adjacent riverbed is experiencing

* Corresponding author: jawadaljabri84@gmail.com; bce.20.14@grad.uotechnology.edu.iq

http://dx.doi.org/10.28991/CEJ-2024-010-08-013

© 2024 by the authors. Licensee C.E.J, Tehran, Iran. This article is an open access article distributed under the terms and conditions of the Creative Commons Attribution (CC-BY) license (http://creativecommons.org/licenses/by/4.0/).

increased incision because of bank protection measures, effectively restricting the lateral erosion of the riverbanks. The maximum erosion depth of 10.6 m occurs over the period from August to November 2020. During field research, laboratory tests were conducted on soils from six riverbanks, revealing properties of the bank soil. The test results reveal that the cohesive bank soils exhibit low dry densities ranging from 1.31 to 1.47 T/m^3 and high-water contents ranging from 28.5% to 40.0%. Additionally, it is seen that the cohesiveness, or angle of internal friction, generally reduces as the water content of the cohesive soil increases [8].

The silt-clay content of banks is an important component in which bank erosion occurs [9]. Hydraulic erosion remains the primary factor causing erosion of protected riverbanks. However, the bank protection mechanism effectively limits the sideways movement of the bank while simultaneously increasing the nearby incision of the riverbed [10]. Studying and understanding the features of soil on riverbanks is crucial for evaluating bank stability and, as a result, the probability of bank retreat. Studies conducted on the soil properties of the Mississippi Riverbank in Goodwin Creek in the United States revealed that the bank consists of multiple sediment layers that have built up over time due to different flood events. The presence of hydraulic conductivity anisotropy, caused by variations in physical and hydraulic properties across various layers, indicates that the movement of water through the soil was not consistent in all directions [4, 11]. The complexity of river systems derives from the interaction of hydrological, sedimentary, and morphological elements. Erosion is a frequent phenomenon in stream banks, although the probability of failure depends on the location and the rate at which erosion takes place. Rivers with banks that are susceptible to erosion generally have a wider width compared to rivers with banks that are more resistant to erosion [12]. Erosion and sedimentation, as natural phenomena, have been continually active throughout geological history, leading to the creation of the current world terrain. Riverbank erosion can cause the deterioration of the riverbed, leading to the accumulation of particles and sediments in the nearby water body. The particles constituting the bedforms, as well as those present in the riverbank, might get dislodged from their interconnected configuration due to the movement of water. The particles will begin movement and settle at the downstream part of a river segment. Inadequate management and implementation of monitoring programs may lead to substantial engineering and environmental difficulties [13].

The study conducted by Aldefae & Alkhafaji [14] analyzed the process by which riverbanks collapse and assessed their resilience under different flow conditions, considering both immediate and prolonged periods. To accomplish this, a series of physical model tests were conducted. The study examined three distinct models and focused specifically on the Tigris River in Iraq. The rate of bank soil erosion decreases as the surface flow velocity decreases. This is logically coherent because the velocity of the water is directly correlated with the magnitude of the force it applies on the shore. A decrease in velocity diminishes the erosive pressures exerted on the bank, resulting in a reduction in the erosion rate. According to Thi & Minh [15], the complexity of bank behavior and the mechanisms causing bank retreat can be influenced by several factors, such as vegetation cover, soil characteristics, and the extent and frequency of flow variations. Hence, to accurately predict and control the stability of banks, it is crucial to possess a comprehensive understanding of the surrounding context. Soil erodibility refers to the capacity of soil to resist erosion. This attribute is determined by multiple factors, such as soil composition, permeability, and organic material concentration. Riverbank erosion can cause silt deposition, hence worsening problems associated with river pollution. The transportability of sediments depends on the velocity of the river's current. The initiation of sediment movement is anxiously anticipated due to the combined influence of velocity, bed form features, and kinetic energy found at the riverbed [16]. When the shear stress applied by the flow exceeds the shear stress encountered by the particles, the particles begin to move [17].

The erosion of bank is a naturally unstable phenomenon. It can generate a wide range of riparian habitats [18]. Previous studies [19, 20 and 21] found that the relationship between the rate at which a riverbank recedes and the depth of water along the bank, as well as the height of the bank, can provide significant insights into the behavior of riverbanks [22]. The findings also indicate an association between the speed at which banks recede and the ratio of bank height to the depth of water near the bank [23, 24]. Upon conducting a thorough analysis of the existing literature, it became evident that there is a lack of previous studies that have investigated erosion on laboratory river banks, particularly in a laboratory setup with a river bank inclined at a 26° angle, to assess erosion under varying flow velocities. The objective of this study is to evaluate the impact of the slope of the riverbanks and the operational flow velocities on the deterioration of stability in the banks of the Al Mowahada channel. This involves creating a physical model to simulate the behavior and replicate the identical conditions encountered in the field to investigate the main variables contributing to bank failure in the region.

2. Implementation Details

2.1. Case Study

This study focuses on Al Mowahada Channel, a significant man-made irrigation channel situated in western Baghdad, Iraq. The Al-Fallujah Barrage branches off into the Al-Yossifia district at coordinates N 44° 10' 24" E 05°

02' 33". From there, it supplies water to the Al-Yossifia, Mahmodiyah, and Latifiyah canals (see Figure 1). The water is extracted from the Euphrates River before it reaches the al-Fallujah barrage. The geometric characteristics of the object are as follows: it has a maximum water depth of 5 meters, a minimum water depth of 1.35 meters, and a bottom width of around 20 m. The prototype had a maximum discharge of 140 m3/s and a minimum discharge of 35 m3/s. Furthermore, as depicted in Figure 2, it exhibits earth banks that periodically experience collapse and slide. The operation system of the channel often leads to significant fluctuations in the water table, ranging from 1.35 to 5 m. It remains at 5 m for a period of five days before decreasing back to 1.35 m for an additional five days [25].

Figure 1. Slope instability in the banks of the channel at falling time

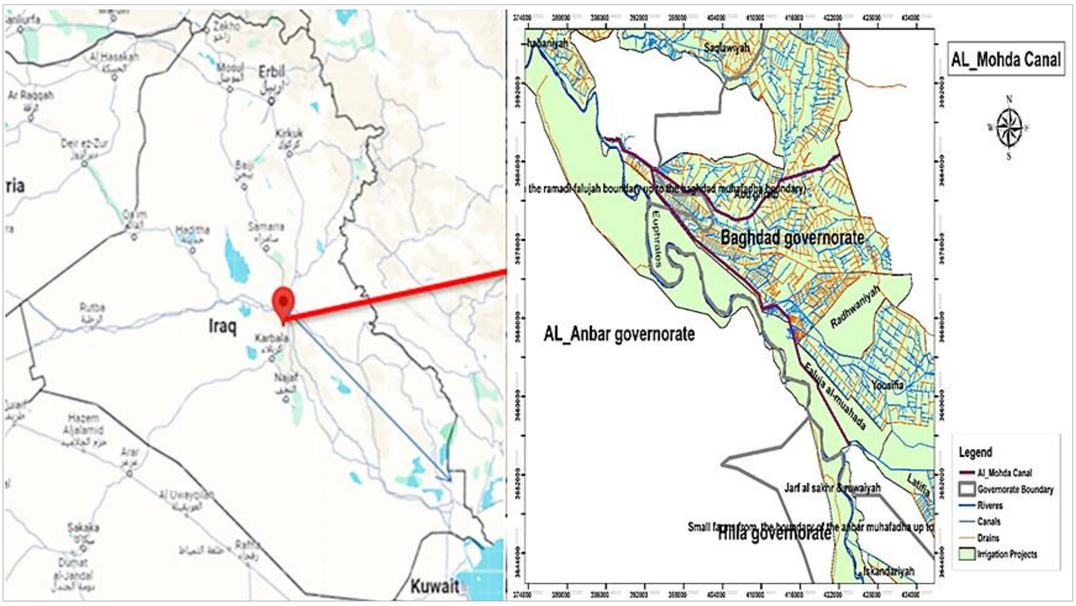

Figure 2. Case study location

The procedure for modeling of channel as follow as:

- Geometric similarity: implies that the ratios of prototype characteristic lengths to model lengths are:

$$Lr = lp/lm = dp/dm = Hp/Hm \tag{1}$$

where l, d and H are the Length, depth and the height, respectively.

- The subscripts p and m refer to prototype (full scale) and model parameters, respectively, and the subscript r indicates the ratio of prototype-to-model quantity. length, area and volume are the parameters involved in geometric similitude.
- Kinematic similarity: implies that the ratios of prototype characteristic velocities to model velocities are the same according to the following equations:

$$Vr = \frac{Vp}{Vm} \tag{2}$$

where V is the velocity.

Let Lr = 45 → scale $=\frac{1}{45}$

$Lr = \frac{Wp}{Wm} \rightarrow 45 = \frac{40}{Wm} \rightarrow Wm = 0.9$ m

where W is the top width of model.

$Lr = \frac{Wp}{Wm} \rightarrow 45 = \frac{20}{Wm} \rightarrow Wm = 0.45$ m.

$Lr = \frac{dp}{dm} \rightarrow 45 = \frac{5}{dm} \rightarrow d_m = 0.11$ m

where M is the max. depth of model.

$Lr = \frac{dp}{dm} \rightarrow 45 = \frac{1.35}{dm} \rightarrow d_m = 0.03$ m Min. depth of model.

Max. discharge of prototype =140 m^3/s

Min. discharge of prototype =35 m^3/s

$Qr = \frac{Qp}{Qm}$, Qr= $L^{5/2} = 45^{5/2} = 13584$

$Qr = \frac{Qp}{Qm} \rightarrow Q_m = 140/13584 = 0.01\ m^3/s$ (10 L/s) Max. discharge for model.

$Qr = \frac{Qp}{Qm} \rightarrow Q_m = 35/13584 = 0.00257\ m^3/s$ Min. discharge for model.

The case study is a trapezoidal channel (prototype), therefore the model also trapezoidal shape Furthermore. Free surface flows (e.g. rivers and wave motion), gravity effects are predominant.

- Model prototype similarity is performed usually with a Froude similitude:

$Fr_p = Fr_m$

If the gravity acceleration is the same in model and prototype, a Froude number modeling implies:

$V_r = Lr^{1/2}$ Froude similitude

Area of prototype channel= $(B+z\ y_0)y_0 = (20+2\times5)5 = 150\ m^2$

$Q_p = V_p \times A_p \rightarrow V_p = Q_p/A_p \rightarrow V_p = 140/150 = 0.933$ m/s. Max. velocity.

Froude number$=\frac{V}{\sqrt{g\times y}} = \frac{0.933}{\sqrt{9.81\times5}} = 0.133$ (for prototype)

Area of model = $(0.45+2\times0.11)\times0.11 = 0.0737\ m^2$

$Q_m = 0.01\ m^3/s$.

$V_m = Q^m/A_m = 0.01/0.0737 = 0.135$ m/s

Froude number of model $=\frac{V}{\sqrt{g\times y}} = \frac{0.135}{\sqrt{9.81\times0.11}} = 0.13 \approx$ Froude number of prototype [26, 27].

2.2. Design of Flume

The laboratory studies were conducted using a lab flume. The flume was created according to the specifications depicted in Figures 3 and 4 in order to provide a physical model that closely mimics the characteristics of a natural channel, while allowing for controlled experimental settings. The flume's basic structure consists of a steel frame with dimensions of 3 m in length, 1 meter in width, and 0.6 meters in depth. In addition, construct soundproof tanks with dimensions of 0.4 m in thickness, 1 m in width, and 1.5 m in height to calm the water flowing from the pump. The flume's side walls are formed with plaxiglass that is 4 mm thick. A steel water tank with a capacity of 1800 liters. The pumping system comprises a pump with a power rating of three horsepower, which is responsible for propelling water into a flowmeter designed in the style of a Rotameter. To quantify the amount of fluid entering the quieting tank, employ this flowmeter. A pipe with a diameter of four inches is used to link the entire pumping system to the flume. The outletting system comprises four ports, each one with 2.5 inches. Each port is equipped with a valve that allows for independent regulation of water output, based on the specific requirements of the experiment. The supply tank collected the water that was returned from the outflow. A sleek plate functioned as the flume bed, which also had a vertical point gauge for the purpose of monitoring the water level in the flume.

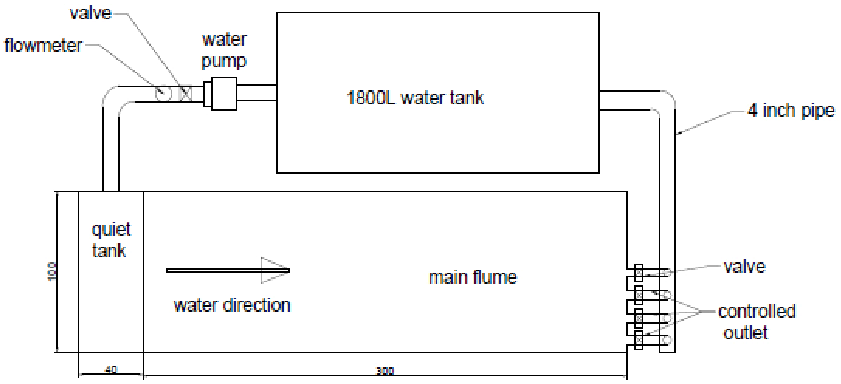

Figure 3. Scheme of the laboratory flume (all dimensions in cm)

Figure 4. The laboratory flume (model)

3. Material and Methods

The flume model is designed to accurately replicate the parameters and conditions of the field and reproduce them in the laboratory. The source sediment from the Al Mowahada canal is used in a controlled laboratory setting to construct the riverbank, taking into consideration the required slope and density of soil. Regulate both the flow velocity and water depth in the experimental flume. The study involves carrying out laboratory experiments by simulating a model in flume, as demonstrated previously. Next, configure riverbanks with a slope angle of 26º. The soil's physical parameters under consideration include specific gravity, dry unit weight, and water content. The physical and chemical characteristics of the soil obtained via the borehole at the riverbank site are presented in Figure 5 and Table 1.

Figure 5. Soil investigations of the embankment

Table 1. Physical and chemical properties of bank soil

Sample Information		Index Properties				Dry Unit Weight	Water Content	Specific Gravity	Direct shear test		Grain Size Analysis			Chemical Tests			
Depth (m)	**Type**	**L.L.**	**P.L.**	**P.I.**	**USCS**	**γ_d, kN/m^3**	**W_C%**	**Gs**	**ckPa**	**ϕ °**	**Clay & Silt %**	**Sand %**	**Gravel %**	**So_3%**	**TSS%**	**Gyp%**	**Org%**
1.5	US	39.4	26.9	12.5	ML	14.4	24.5	2.69	17.1	29.4	62.8	37.2	0.0	0.91	11.3	1.94	3.87
General Description: Light brown sandy silt mixed with white crystals of salts and some organic matters and roots of plants.																	
3.0	US	38.8	27.1	11.7	ML	14.5	25.9	2.68	15.3	28.2	67.1	32.9	0.0	0.72	10.4	1.54	4.09
General Description: Light brown sandy silt mixed with white crystals of salts and some organic matters and roots of plants.																	
4.5	SPT	NP	NP	NP	SP	15.0	32.7	2.66	1.7	33.6	98.7	1.3	0.0				
General Description: Gray sand.																	
6.0	SPT				CL		33.6							0.71	9.88	1.52	7.98
General Description: Greenish light brown clay mixed with white crystals of salts and organic matters.																	
7.5	SPT	NP	NP	NP	ML		33.7				56.3	43.7	0.0				
General Description: Brown to gray sandy silt.																	
9.0	D.S						27.9										
General Description: Brown to gray clay.																	
10.5	D.S	47.5	26.5	21.0	CL		28.4	2.72			100.0	0.0	0.0				
General Description: Brown to gray clay.																	
12.0	D.S	46.3	26.1	20.2	CL		27.8				100.0	0.0	0.0				
General Description: Brown to gray clay.																	

Figure 6 shows the flowchart of the research methodology through which the objectives of this study were achieved.

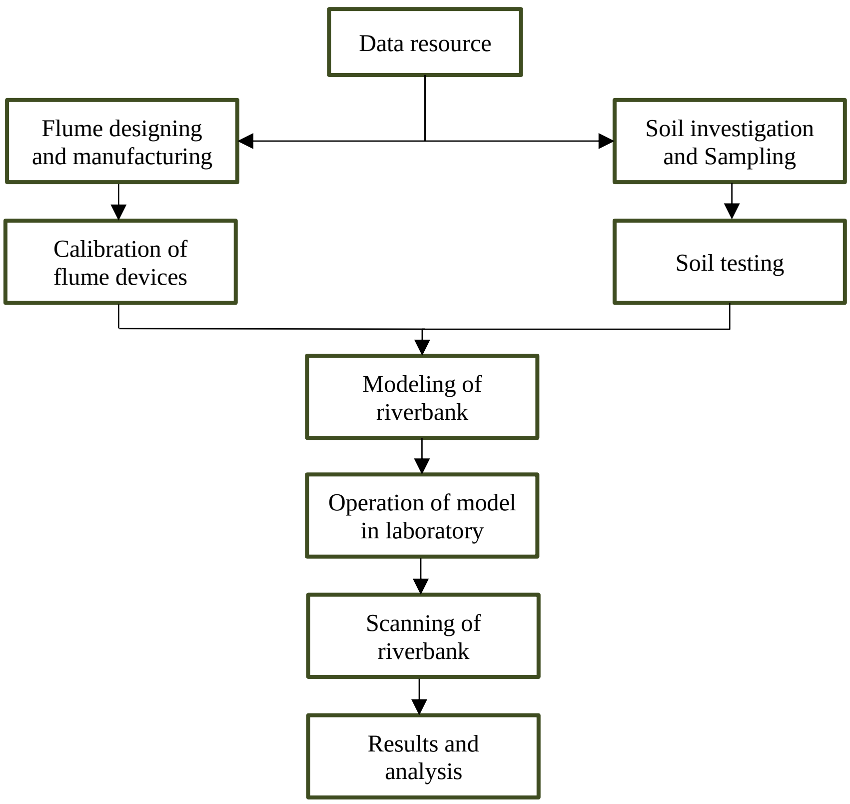

Figure 6. Flowchart shows the process of the methodology

4. Soil Preparation

The soil preparation, which was the most crucial component of the work in the laboratory, was divided into three distinct stages:

Firstly, the procedure of soil sampling involves extracting a soil sample from one side of a bank channel. This sample should be taken from a location that is in direct contact with the failure region, specifically a distance of 1.5 meters below the surface soil and half a meter above the top layer of bank soil. The upper most stratum comprised a depth of 5 m of silty sand soil. The process of soil drying entails dispersing a soil sample onto a nylon sheet, which is then folded into a single layer around 10 cm thick and exposed to the open air for natural evaporation.

Secondly, it is important to ensure that the soil sample exhibits a uniform gradient. The soil sample was compacted by penetrating it with an iron rod and subsequently passed through a filtering device with a pore size of 4.5 mm.

Thirdly, it is crucial to ensure that the soil water content in both the field and the laboratory closely mirrors the real circumstances found in the field. After the soil was allowed to dry naturally, the water content of the sample decreased to 13%, as depicted in Figure 7. The sand layer in the field has a water content of 32.7%. The soil's weight was measured, and the weight of the mold was subtracted to obtain the net weight of the soil. To obtain the field water content, a precise quantity of water must be applied to the soil sample. After multiple trials, it was determined that the optimal water ratio for the soil sample is 25.2% based on its weight [28, 29].

Figure 7. Spread, smoothing and drying of soil sample

5. Experimental Setup

The slope angle of riverbank 26° is used, as shown in Figure 8, the geometric information presented in Table 2. The slope angle was associated with five distinct velocities, which were arranged in an ascending sequence as shown in Table 3. At each velocity, the bank deformation is measured at two locations, with data points gathered at fixed intervals of 3 hours (3, 6, 9, and 12). The first station is positioned 1.2 m from the inlet point, while the second station is positioned 1.7 m away. A single measurement entails employing a laser scanner to scan the cross-section of the riverbank and determine the distortions caused by erosion resulting from the flow velocity. One side of the river was used in these experiments.

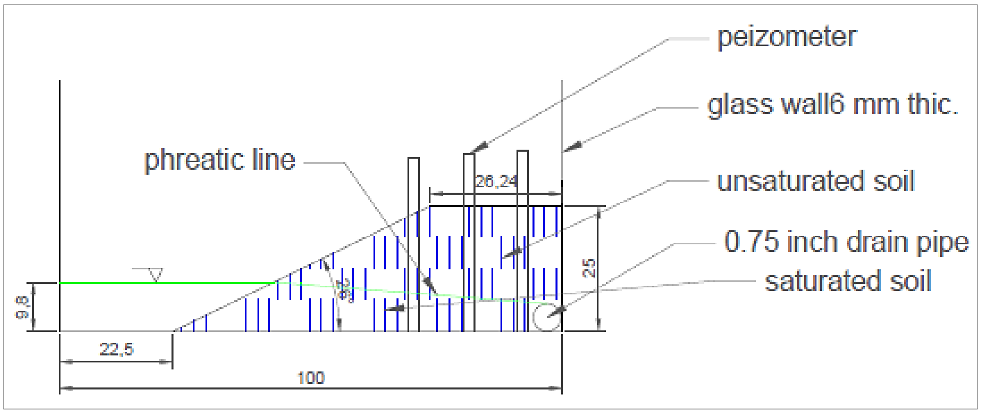

Figure 8. River bank model in flume

Table 2 . Geometry of laboratory bank after modeling the actual

Geometry of bank in (cm)				
Bank angle	**Length of bank**	**Width of bottom**	**Width of top**	**height**
26°	200	77.5	26.24	25

Table 3. Laboratory angles and corresponding experiment velocities by modeling the actual velocities in field

No.	Angle	Velocity (m/s)				
		EXP.1	**EXP.2**	**EXP.3**	**EXP.4**	**EXP.5**
1	26°	0.101	0.116	0.12	0.13	0.135

Three piezometers were located at regulated distances, both longitudinally and transversely, within the bank. These piezometers are utilized to monitor the water level within the bank. A 0.75 inch perforated plastic pipe was added to collect water from inside the bank and drain it outside the flume in order to simulate the original state bank (see Figure 9).

Figure 9. Prepare the model for scanning and reduce the water level in the flume

6. Results and Discussion

This study investigated the effect of erosion on the soil of a riverbank due to the energy generated by the velocity of water flow and the slope angle. The experiment commenced by supplying a flow with a velocity of 0.101 m/s into the flume, which had a riverbank angle of 26° in the laboratory. The experiment persisted for a continuous duration of 12 hours. A laser scanner was employed to scan the bank at regular intervals of three hours; four results were provided for each velocity. The post-operation analysis revealed that the erosion was minimal due to two factors: firstly, the slope angle of the bank was more stable, and secondly, the flow velocity was low. Figure 10 and Table 4 provide graphs and numerical representations of the erosion amounts. Despite being limited in scope, there is a significant amount of erosion occurring in the central portion of the bank. The most significant impact occurred near the surface of water. The foundation of the bank experienced the least impact at this velocity.

The local erosion exhibits a high rate throughout the initial phases of the experiment, especially within the first six hours of the flow. As the scouring process proceeds, it gradually decreases until it reaches a state of equilibrium, due to the influence of the erosive activity at the bed.

The erosion in the second velocity (0.116 m/s) is clearly apparent, particularly in the lower third of the bank. The erosion increases as it approaches the surface of the flow, as depicted in Figure 11 and Table 5. At this velocity, the impact starts three centimeters above the bottom of the flume and gradually intensifies as it reaches the surface of the water. After 6 hours of the experiment, there is a significant increase in erosion, which is clearly visible above the depth of 4.5 cm from the bottom of the flume.

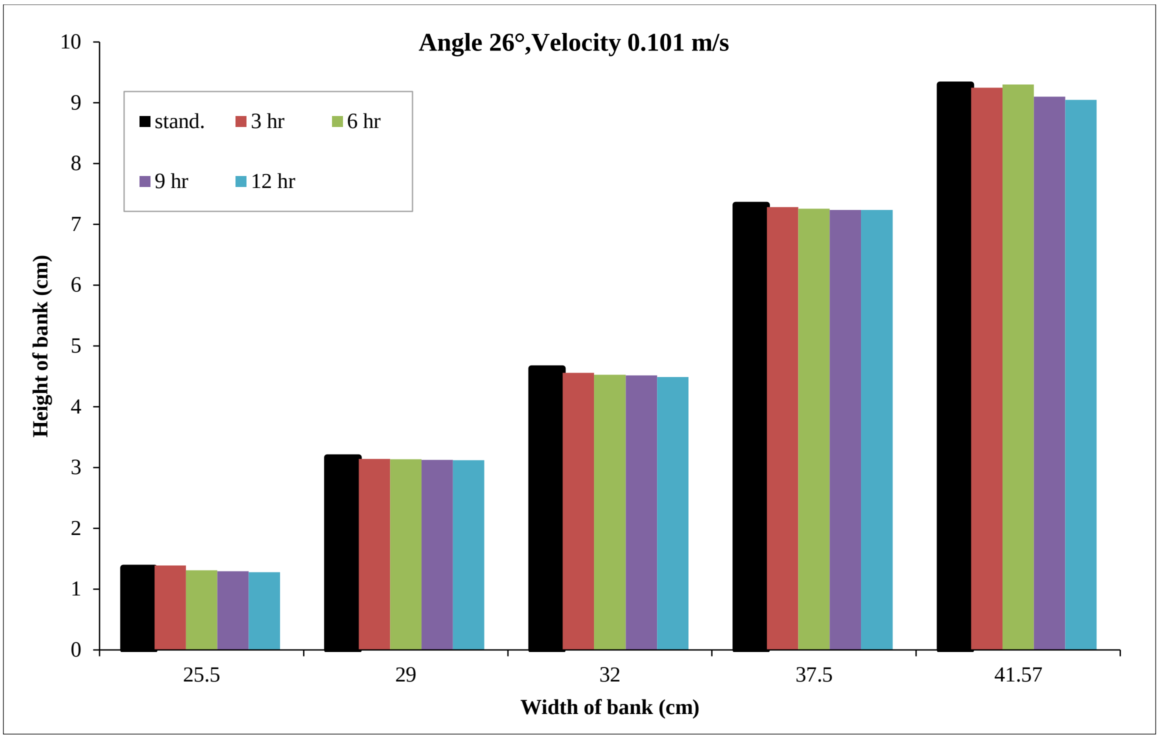

Figure 10. The erosion in the bank river with flow velocity 0.101 m/s and slope angle 26°

Table 4. Amounts of erosion for riverbank with 26° slope, and velocity 0.101 m/s (in cm)

Scan of bank before running	Scan of bank after running	Erosion amounts
1.35	1.28	0.07
3.17	3.12	0.05
4.63	4.49	0.14
7.32	7.235	0.085
9.3	9.05	0.25

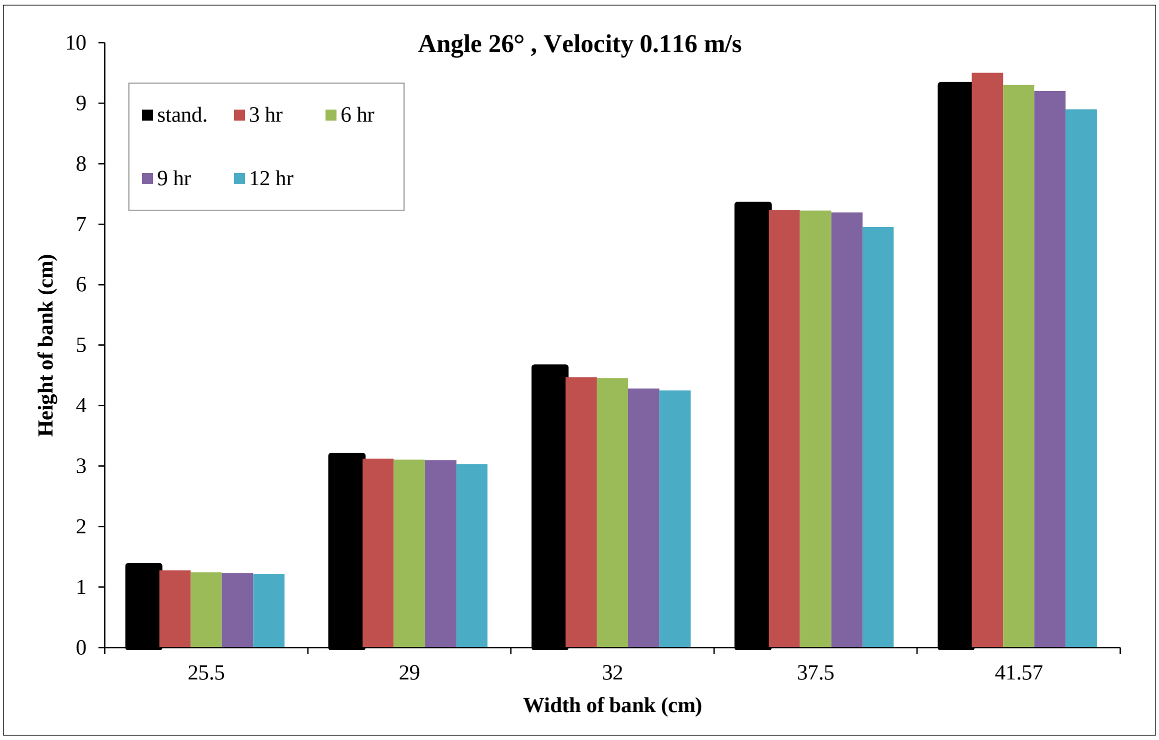

Figure 11. The erosion in the bank river with flow velocity 0.116 m/s and slope angle 26°

Table 5. Erosion for riverbank with 26° slope and velocity 0.116 m/s (in cm)

Scan of bank before running	Scan of bank after running	Erosion amounts
1.35	1.22	0.13
3.17	3.035	0.135
4.63	4.25	0.38
7.32	6.95	0.37
9.3	8.9	0.4

However, when the velocity reached 0.12 m/s, there was a notable increase in the quantity of erosion compared to the prior two velocities. Erosion progressively increases as the height decreases from the bottom of the flume towards the water surface. The erosion rate increased by approximately 45% when the flow velocity increased from 0.116 m/s to 0.12 m/s compared to the previous velocity. The erosion of the riverbank led to an increase in the cross-sectional area of the flow, and because the flow discharge was constant during the experiments, this caused a decrease in the water level inside the flume, as shown in Figure 12 and Table 6. The sediment generated from the erosion of the river bank will inevitably be deposited at the bottom of the flume, as depicted in Figure 12.

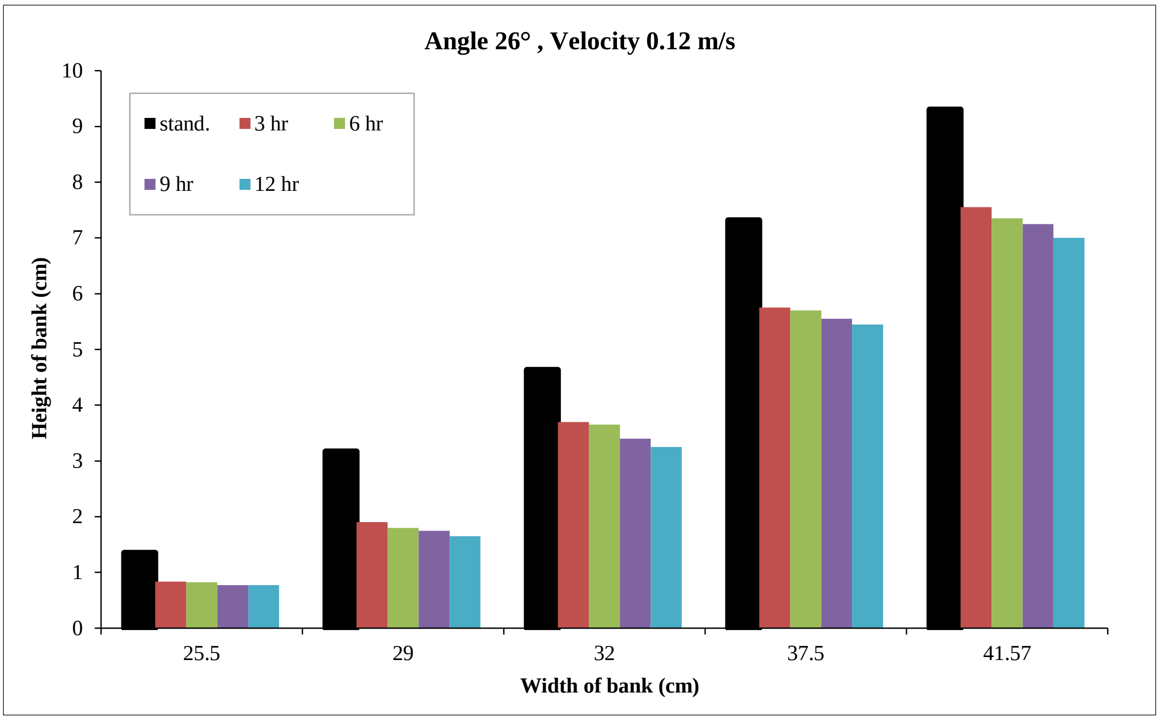

Figure 12. The erosion in the riverbank with flow velocity 0.12 m/s and slope angle 26º

Table 6. Erosion of riverbank with 26° slope angle and velocity of 0.12 m/s (in cm)

Reading of bank before running	Reading of bank after running	Erosion amounts
1.35	0.77	0.58
3.17	1.65	1.52
4.63	3.25	1.38
7.32	5.45	1.87
9.3	7	2.3

At a velocity of 0.13 m/s, the erosion quantity experienced a significant rise, as depicted in Figure 13 and Table 7. This increase in erosion was directly related to the increase in cross-sectional area of the flume, which resulted from the deformation occurring in the bank. The enlargement of the cross-sectional area of the channel has an impact on the hydraulic characteristics of the channel. Furthermore, the velocity distribution curve within the channel underwent alteration. The experiment reveals that the deformation in the canal bank is consistently even, resulting in a minimal alteration in the estimated angle of inclination of the bank. This indicates that angle 26º is stable, although it does not effectively decrease erosion.

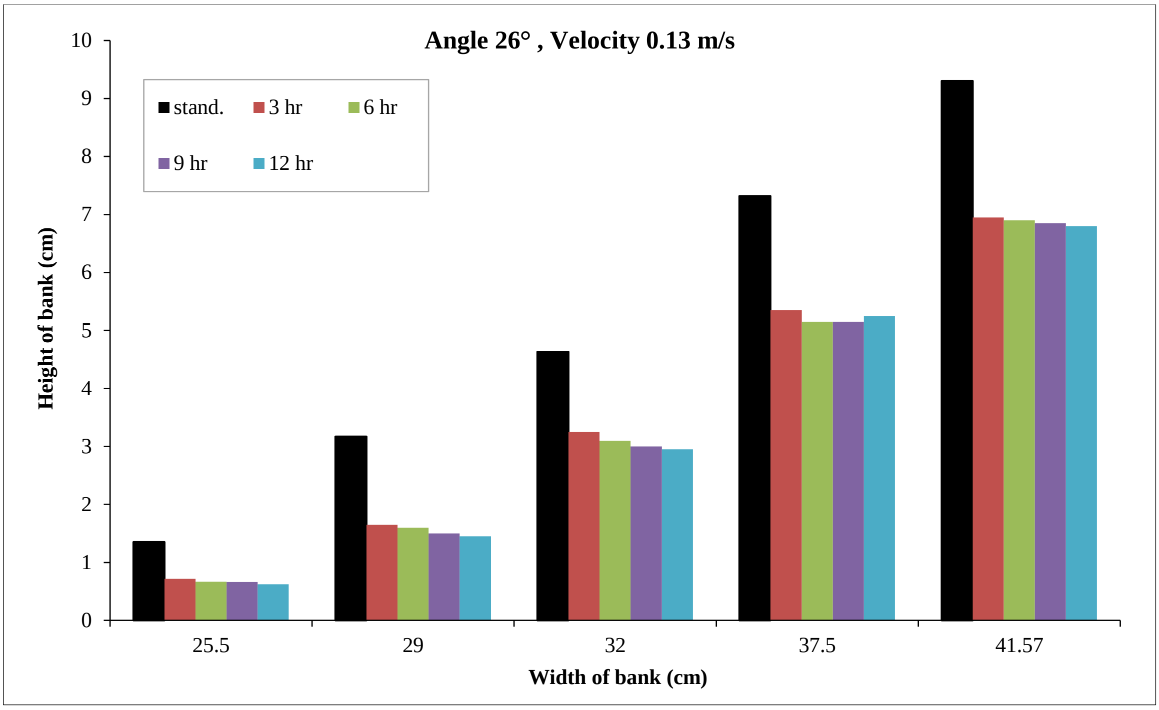

Figure 13. The erosion in the bank river with flow velocity 0.113 m/s and slope angle 26º

Table 7. Erosion for riverbank with 26° slope and velocity of 0.13 m/s (in cm)

Reading of bank before running	Reading of bank after running	Erosion amounts
1.35	0.62	0.73
3.17	1.45	1.72
4.63	2.95	1.68
7.32	5.25	2.07
9.3	6.8	2.5

Regarding the velocity of 0.135 m/s, the amount of erosion in the bank remained relatively consistent compared to the preceding velocity, as depicted in Figure 14 and Table 8.

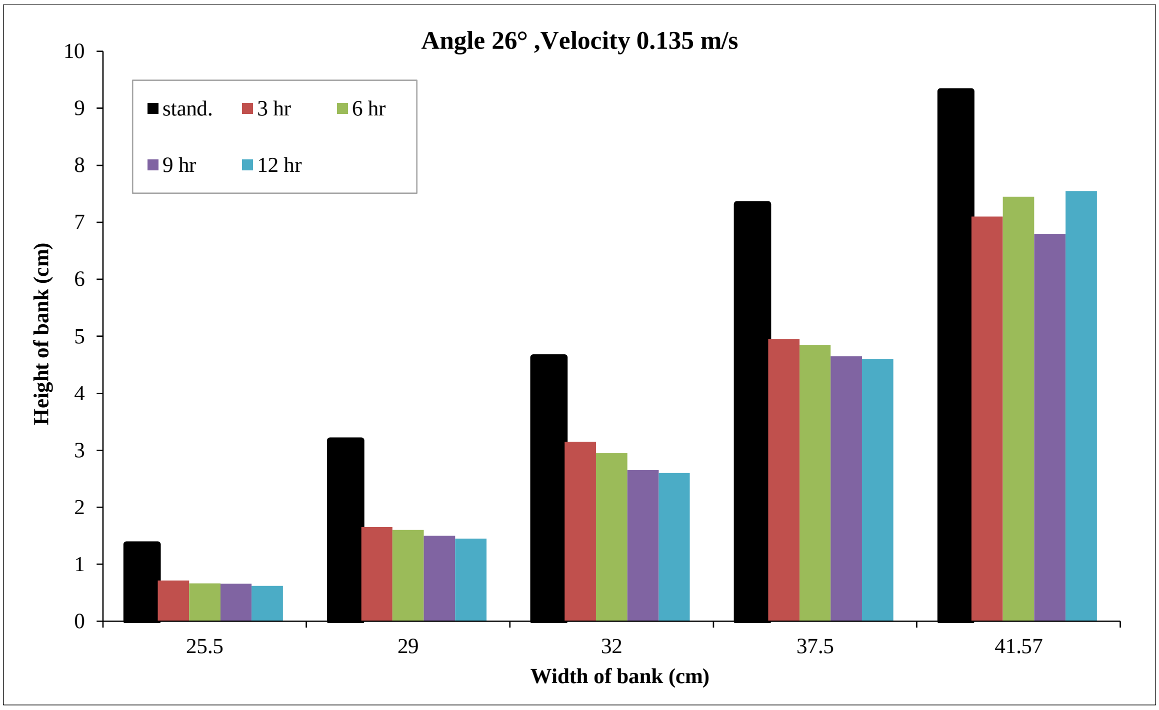

Figure 14. The erosion in the riverbank with flow velocity 0.135 m/s and slope angle 26º

Table 8. Erosion for riverbank with 26° slope and velocity of 0.135 m/s (in cm)

Reading of bank before running	Reading of bank after running	Erosion amounts
1.35	0.62	0.73
3.17	1.45	1.72
4.63	2.6	2.03
7.32	4.6	2.72
9.3	8.95	0.35

Through the discussion and analysis of the aforementioned facts, a correlation was established between the deformation in the shape of the bank and the velocity, as depicted in Figure 15.

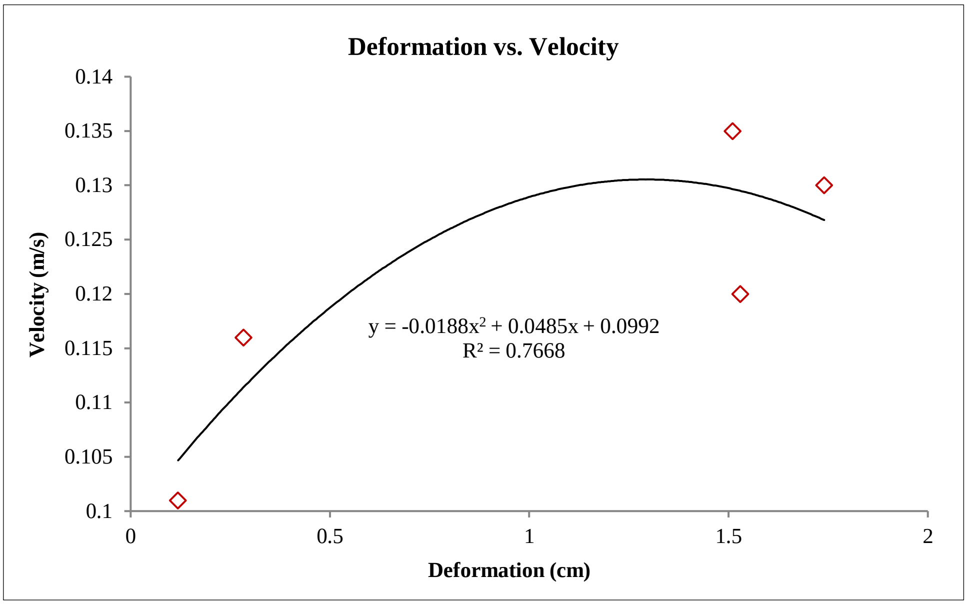

Figure 15. Relationship between the velocity of flow vs. the deformation in the riverbank

7. Conclusions

This study aimed to investigate the phenomenon of riverbank stability in relation to erosion by assessing experimental data obtained from laboratory work. A laboratory flume with dimensions of 3 m in length, 1 m in width, and 0.6 m in height was utilized. Additionally, soil samples were obtained from the original bank of the case study, a soil investigation was conducted, and laboratory testing on the soil samples gathered from the riverbank was performed. A riverbank was constructed within the flume at a 26º inclination. A laboratory setup was not previously constructed to examine erosion under varying flow velocities on a riverbank inclined at an inclination of 26°. A range of flow velocities was selected, starting from the minimum velocity of the original channel and ending with its maximum velocity following the modeling procedure. The experiment runs for a duration of 12 hours at each velocity, with data being recorded at three-hour intervals. The reading is obtained by using a laser to scan the bank in a direction that is perpendicular to the bank section. This scanning process is done for two stations at a time. The study's main findings suggest that a reduction in flow velocity results in a corresponding decrease in erosion volume.

The study revealed that a riverbank with a slope of 26º exhibits greater resistance to erosion while the velocity of the flow remains below 0.12 m/s. Erosion intensifies when the flow velocity surpasses 0.12 m/s. Erosion primarily occurs in the upper two-thirds of the bank. The angle of 26° is stable; however, it does not mitigate erosion. According to the study, riverbank erosion increases in laboratory conditions when the velocity reaches 0.12 m/s or higher. This is equivalent to a velocity of 0.804 m/s in the prototype. The upper two-thirds of the riverbank is the most severely affected area by erosion. The study conducted by Nama et al. [30] demonstrates the reach morphology's susceptibility to changes in flow brought about by any change in flow velocity of flow regime. This supports the research results that the river banks are the most affected by any hydraulic change.

In conclusion, to gain a deeper understanding of erosion in bank slope canals, additional research will be undertaken in the future for slop angles of 45° and 60°.

8. Declarations

8.1. Author Contributions

Conceptualization, J.K.M. and H.A.H.; methodology, J.K.M. and H.A.H. formal analysis, J.K.M.; investigation, J.K.M., H.A.H., and S.F.A.; resources, J.K.M.; data curation, J.K.M.; writing—original draft preparation, J.K.M.; writing—review and editing, J.K.M. and S.F.A.; visualization, J.K.M.; supervision H.A.H. and M.Q.W.; funding acquisition, J.K.M. All authors have read and agreed to the published version of the manuscript.

8.2. Data Availability Statement

The data presented in this study are available on request from the corresponding author.

8.3. Funding and Acknowledgements

The authors would like to thank the technical and faculty staff of the Civil Engineering Department at the University of Technology, Baghdad, Iraq, for their valuable support and scientific assistance.

8.4. Conflicts of Interest

The authors declare no conflict of interest.

9. References

[1] Thorne, C. R., & Lewin, J. (2020). Bank processes, bed material movement and planform development in a meandering river. Adjustments of the fluvial system. Routledge, Milton Park, United Kingdom.

[2] Darby, S. E., & Thorne, C. R. (1996). Numerical Simulation of Widening and Bed Deformation of Straight Sand-Bed Rivers. I: Model Development. Journal of Hydraulic Engineering, 122(4), 184–193. doi:10.1061/(asce)0733-9429(1996)122:4(184).

[3] Millar, R. G. (2000). Influence of bank vegetation on alluvial channel patterns. Water Resources Research, 36(4), 1109–1118. doi:10.1029/1999WR900346.

[4] Simon, A., Curini, A., Darby, S. E., & Langendoen, E. J. (2000). Bank and near-bank processes in an incised channel. Geomorphology, 35(3–4), 193–217. doi:10.1016/s0169-555x(00)00036-2.

[5] Goodson, J. M., Gurnell, A. M., Angold, P. G., & Morrissey, I. P. (2002). Riparian seed banks along the lower River Dove, UK: Their structure and ecological implications. Geomorphology, 47(1), 45–60. doi:10.1016/S0169-555X(02)00140-X.

[6] Eaton, B. C., Church, M., & Millar, R. G. (2004). Rational regime model of alluvial channel morphology and response. Earth Surface Processes and Landforms, 29(4), 511–529. doi:10.1002/esp.1062.

[7] Deng, S., Xia, J., Zhou, Y., Zhou, M., & Zhu, H. (2024). Prediction and early-warning of bank erosion in the Middle Yangtze River, China. Catena, 242, 108105. doi:10.1016/j.catena.2024.108105.

[8] Xia, J., Zong, Q., Deng, S., Xu, Q., & Lu, J. (2014). Seasonal variations in composite riverbank stability in the Lower Jingjiang Reach, China. Journal of Hydrology, 519, 3664–3673. doi:10.1016/j.jhydrol.2014.10.061.

[9] Julian, J. P., & Torres, R. (2006). Hydraulic erosion of cohesive riverbanks. Geomorphology, 76(1–2), 193–206. doi:10.1016/j.geomorph.2005.11.003.

[10] Zhou, Y., Xia, J., Deng, S., & Han, Z. (2024). Bank erosion under the impacts of hydraulic erosion, river stage change and revetment protection in the Middle Yangtze River. Geomorphology, 448, 109043. doi:10.1016/j.geomorph.2023.109043.

[11] Thorne, C. R., & Tovey, N. K. (1981). Stability of composite river banks. Earth Surface Processes and Landforms, 6(5), 469–484. doi:10.1002/esp.3290060507.

[12] Darby, S. E., & Thorne, C. R. (1996). Development and Testing of Riverbank-Stability Analysis. Journal of Hydraulic Engineering, 122(8), 443–454. doi:10.1061/(asce)0733-9429(1996)122:8(443).

[13] Julien, P. Y. (2010). Erosion and sedimentation. Cambridge University Press, Cambridge, United Kingdom. doi:10.1029/EO052i006pIU292.

[14] Aldefae, A. H., & Alkhafaji, R. A. (2021). Experimental and numerical modeling to investigate the riverbank's stability. SN Applied Sciences, 3(2), 164. doi:10.1007/s42452-021-04168-5.

[15] Duong Thi, T., & Do Minh, D. (2019). Riverbank Stability Assessment under River Water Level Changes and Hydraulic Erosion. Water, 11(12), 2598. doi:10.3390/w11122598.

[16] Yang, C. T. (2006). Reclamation: Managing Water in the West Denver. Technical Service Center, Sedimentation and River Hydraulics Group, Bureau of Reclamation, US Department of Interior, Colorado, United States.

[17] Sulaiman, M. S., Sinnakaudan, S. K., & Shukor, M. R. (2013). Near bed turbulence measurement with acoustic doppler velocimeter (ADV). KSCE Journal of Civil Engineering, 17(6), 1515–1528. doi:10.1007/s12205-013-0084-8.

[18] Florsheim, J. L., Mount, J. F., & Chin, A. (2008). Bank erosion as a desirable attribute of rivers. BioScience, 58(6), 519-529. doi:10.1641/B580608.

[19] Zhao, K., Gong, Z., Zhang, K., Wang, K., Jin, C., Zhou, Z., Xu, F., & Coco, G. (2020). Laboratory Experiments of Bank Collapse: The Role of Bank Height and Near-Bank Water Depth. Journal of Geophysical Research: Earth Surface, 125(5), 2019 005281. doi:10.1029/2019JF005281.

[20] Maatooq, J. S., & Alkhafaji, H. (2022). Field Study of the Differential Movements Problems for the Construction Joints of Al-Shamiya Barrage -South of Iraq. Proceedings of the 39th IAHR World Congress, 2756–2764. doi:10.3850/iahr-39wc2521711920221.

[21] Abdulwahd, A. K., & Maatooq, J. S. (2023). Experimental investigation of local scour under two oblong piers of a bridge crossing a sharp bend river. Journal of Water and Land Development, 58, 129–135. doi:10.24425/jwld.2023.146605.

[22] Abdulwahd, A., & Maatooq, J. (2023). Effect of Bridge Piers Locations and Flow Intensity on Morphological Change in a 180-Degree River Bend. Engineering and Technology Journal, 41(11), 1–11. doi:10.30684/etj.2023.140134.1455.

[23] Maatooq, J. S., & Adhab, B. A. (2017). Effect of Distance of the Submerged Vanes from the Outer Bank on Sediment Movement within 180° Bend. American Journal of Engineering and Applied Sciences, 10(3), 679–684. doi:10.3844/ajeassp.2017.679.684.

[24] Abbass, Z. D., Maatooq, J. S., & Al-Mukhtar, M. M. (2023). Monitoring and Modelling Morphological Changes in Rivers Using RS and GIS Techniques. Civil Engineering Journal (Iran), 9(3), 531–543. doi:10.28991/CEJ-2023-09-03-03.

[25] MOWR (2024). Ministry of water resources/ directorate of water resources of Abu-Ghareeb-Iraq (2022). Ministry of Water Resources, Baghdad, Iraq.

[26] Chanson, H. (2004). Hydraulics of open channel flow. Elsevier, Amsterdam, Netherlands.

[27] Samadi, A., Amiri-Tokaldany, E., Davoudi, M. H., & Darby, S. E. (2013). Experimental and numerical investigation of the stability of overhanging riverbanks. Geomorphology, 184, 1–19. doi:10.1016/j.geomorph.2012.03.033.

[28] Amiri-Tokaldany, E., Dovoodi, M. H., Darby, S. E., & Taghavi, M. (2010). A method to estimate failure plane angle and tension crack depth. Conference Paper on River Flow 2010. Karlsruhe: Bundesanstalt für Wasserbau, 1293-1300.

[29] Jamal, M., Khatun, S., Jha, S., Mehta, D., Dixit, S., Kumar, V., & Tiwari, D. K. (2024). Experimental investigation of the efficiency of stone revetment for different temporal variations with the static water condition. Journal of Water and Climate Change, 15(4), 1969–1980. doi:10.2166/wcc.2024.126.

[30] Nama, A. H., Abbas, A. S., & Maatooq, J. S. (2022). Field and Satellite Images-Based Investigation of Rivers Morphological Aspects. Civil Engineering Journal (Iran), 8(7), 1339–1357. doi:10.28991/CEJ-2022-08-07-03.